Metastability of single-bonded cubic-gauche structure of N under ambient pressure

T. Zhang, S. Zhang, Q. Chen, and L.-M. Peng*
Key Laboratory for the Physics and Chemistry of Nanodevices and Department of Electronics, Peking University, Beijing 100871, China
(Received 1 June 2005; revised manuscript received 6 January 2006; published 3 March 2006)

A density functional theory investigation is carried out to determine whether or not the cubic-gauche nitrogen (cg-N) crystal is mechanically stable under ambient pressure. Phonon dispersion surface calculations show that an infinite cg-N crystal is metastable under ambient pressure. The surface stability and effect of surface passivation using hydrogen atoms were also examined. It was found that the (110) surface of cg-N is the least stable surface among the three low-index surfaces investigated, i.e., (100), (110), and (111), and the surface stability of these surfaces may be improved by passivating the surface dangling bonds with hydrogen atoms.

DOI: 10.1103/PhysRevB.73.094105 PACS number(s): 63.20.−e, 64.70.−p, 68.35.−p

I. INTRODUCTION

Under usual conditions, the most stable form of nitrogen is the molecular form, which contains two nitrogen atoms with a triple bond between them. Nitrogen molecules condense to a molecular crystal under low temperature because of the van der Waals interaction between them. But under high pressure nitrogen molecules are predicted to transform to an atomic solid with a single-bonded crystalline structure.[1] The single-bonded nitrogen is interesting because it could be used as a high-energy-density material. It is well known that the N≡N triple bond is one of the strongest chemical bonds in the world. When the single-bonded nitrogen transforms into N_2 molecules, an energy of about 1 eV/atom can be released, and this is much more efficient than the most powerful energetic materials. However, this potential application depends first on whether or not the material is metastable under the usual conditions, and this paper aims to investigate the metastability of the single-bonded nitrogen material.

Theoretical study shows that the polymeric nitrogen should have an unusual cubic-gauche (cg-N) lattice structure[2] (see Fig. 1). In recent experiments[3–5] the predicted cg-N structure was successfully synthesized under extreme conditions[3] (115 GPa, 2600 K), and its properties were measured. In order to utilize the cg-N material it is important to know the stability of this material and how to further stabilize it under the usual conditions, and to the best of our knowledge this is still an open question. Eremets *et al.*[3] observed that cg-N is at least metastable at room temperature and under 42 GPa, or at 140 K and 25 GPa. Barbee[6] carried out density functional theory (DFT) calculations on the phonon dispersion surface down to 12 GPa and Mailhiot *et al.*[2] obtained a potential barrier of 0.86 eV/atom for the transition from cg-N to a β-O_2 structure under ambient pressure, and these calculations indicate that the cg-N structure does have a certain inherent stability. However, in the work of Mailhiot *et al.*[2] only one possible transition path was considered, and in the work of Barbee[6] no phonon dispersion surface was calculated under ambient pressure. The metastability of cg-N remains therefore unproven. In particular the surface of cg-N has not been considered, while it is well known that the surface plays an important role in considering the metastability of a real crystal. In this paper we carried out DFT calculations, including a phonon dispersion calculation under ambient pressure, and a transition state (TS) search of surface decomposition processes.

II. METHODS

A. Overview

All calculations reported in this paper were performed by using the DFT method with a plane-wave basis set and the CASTEP code.[7] Because cg-N is a typical covalent crystal the generalized gradient approximation for the exchange-correlation (XC) energy was used instead of the simpler local density approximation. We used the widely applied Perdew-Wang form[8] for dealing with the XC effect. For phonon dispersion calculations we employed the norm-conserving pseudopotential,[9] while for transition state search calculations we employed the ultrasoft pseudopotential in its real space representation[10,11] for its superior computational effi-

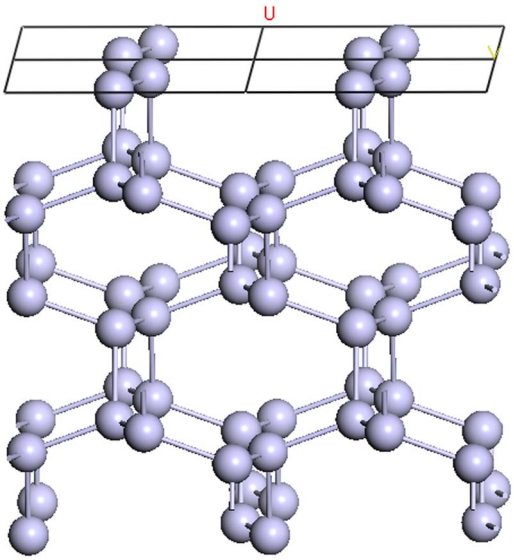

FIG. 1. (Color online) The structure of cubic-gauche nitrogen (cg-N). The lattice has a space group of $I213$, and the nitrogen atoms bond with each other via single bonds.

TABLE I. Geometry parameters of cg-N (LC, lattice constant; AP, atom position in fractional coordinates (x,x,x), BL, bond length; BA, bond angle) under 115.4 GPa, calculated using ultrasoft pseudopotential in reciprocal space representation, ultrasoft pseudopotential in real space representation, and norm-conserving pseudopotential with reciprocal space representation, which are compared with experiment data of Ref. 3.

	LC (Å)	AP	BL (Å)	BA (deg)
Expt.	3.4542	0.067	1.346	108.84
Ultrasoft reciprocal space	3.4958	0.073	1.337	110.75
Ultrasoft real space	3.4967	0.074	1.337	110.82
Norm conserving	3.5070	0.071	1.350	110.10

ciency in dealing with large systems. The performance of the three kinds of pseudopotentials was checked, and we found that all of them gave good results (see Table I). Errors resulting from the transformation between real and reciprocal space representations of the pseudopotential in all transition state search calculations are fount to be quite small and negligible. Because nitrogen atoms do not have *p* or *d* electrons in their core region to screen the nuclear Coulomb potential, the use of the norm-conserving pseudopotential requires the use of a large plane-wave cutoff energy, and in our case 900 eV was used as the cutoff.[6]

B. Phonon dispersion surface

A real crystal should be mechanically stable, which requires, for small motion of each atom, the existence of a restoring force pointing to the corresponding equilibrium position. This requirement is equivalent to the statement that all the phonon frequencies $\omega_{q,\lambda}$ calculated for wave vector **q** and polarization λ must satisfy $\omega^2_{q,\lambda}>0$ throughout the Brillouin zone, except for the acoustic modes at the Γ point, where they should be zero. If an atomic configuration of the crystal is not at its local energy minimum then the force acting on atoms will point in the direction that reduces the system energy. If there exists no local energy minimum, a phase change will occur in the crystal. As a result, for some **q** and polarization λ in the Brillouin zone, one or more phonon frequencies $\omega^2_{q,\lambda}$ may become negative. Practical phonon dispersion calculation schemes have been reviewed in Ref. 12; these methods include the analytical method, supercell method, and linear response method.[12] The analytical method is applicable only if the system energy expression is simple enough to allow for a direct evaluation of the second derivatives of the energy with respect to atomic displacements. The supercell method and the linear response method are applicable in a much wider area. In this work we used the linear response method implemented in the CASTEP code. This method seeks to evaluate the dynamical matrix directly for a set of **q** vectors. The starting point of the linear response approach is evaluation of the second-order change in the total energy induced by atomic displacements. The main advantage of the scheme, compared with the supercell method, is that there is no need to artificially increase the cell size in order to accommodate small values of **q** vectors, as in the frozen phonon method, or to overcome the long-range interaction problem.

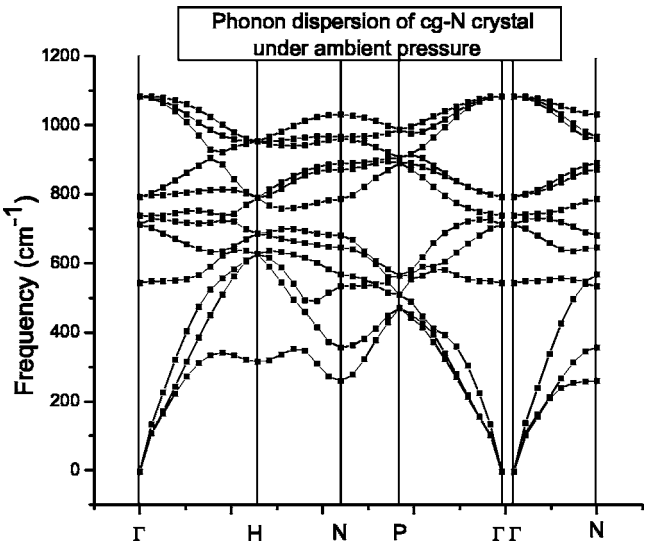

FIG. 2. Calculated phonon dispersion curves of cg-N crystal under ambient pressure. The direction of the **q** vector is listed in Table II.

C. Transition state search

In this section we are concerned with possible surface decomposition processes of cg-N at ambient pressure. It is well known that the breaking of lattice periodicity at the surface causes the appearance of unsaturated surface atoms with dangling bonds. These dangling bonds are energetic and chemically active. The increased energy will cause surface reconstruction and may weaken the coupling between surface atoms and that beneath the surface.

We performed a series of calculation on possible decomposition reaction occurring on low-index surfaces, searched the potential isosurface for determining the transition state and the barrier of crystal surface decomposition. The scheme we employ to search the potential surface via reaction coordinate is called the linear synchronous transit (LST) method.[13] It is a common method for interpolating geometrically between a reactant and a product to generate a reaction pathway. It can be used, in conjunction with single-point energy calculations, to perform transition state searches. The CASTEP code can bracket the LST maximum in the linear interpolated reaction path, and then begin a restricted conjugate gradient minimization process automatically to locate a transition state. The automatical search for the saddle point in the potential surface makes the transition state search task much easier than a manual search. Readers should be reminded that the real surface decomposition process is quite complex. Surface steps, edges, etc. will all influence the decomposition process. Here we are interested only in the metastability of a perfect cg-N crystal, and only ideal surfaces are considered here for theoretical simplicity. Since it is not easy to accurately calculate the energy values when searching for transition states, the transition barriers calculated here are not very accurate and should be regarded as

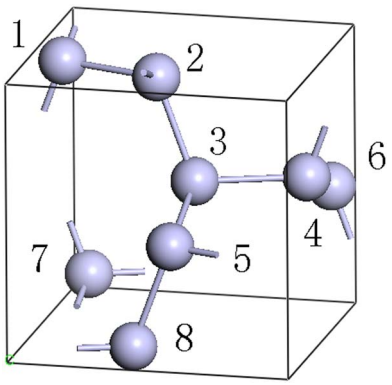

FIG. 3. (Color online) Atomic model showing nonequivalent N atoms in cg-N.

somewhat qualitative rather than quantitative. Nevertheless, as shown in the following section the relative values of the decomposition barrier associated with different subsurfaces do reflect certain important trends of the surface stability of cg-N.

III. RESULTS AND DISCUSSION

A. Phonon dispersion surface of cg-N calculated under ambient pressure

Under ambient pressure, the cg-N lattice was optimized with an optimization convergence tolerance of 5×10^{-6} eV/atom. Relevant geometric parameters of the optimized configuration using the ultrasoft pseudopotential in reciprocal space representation are as follows: lattice constant $a_0=3.81$ Å, atom position $x=0.089$, N—N single bond length=1.402 Å, and bond angle=115.033°. With the same accuracy the optimized cg-N configuration using the norm-conserving pseudopotential has the following parameters: $a_0=3.84$ Å, $x=0.071$, N—N single bond length=1.43 Å, and bond angle=113.833°. These two sets of parameters are rather close, indicating that the two pseudopotentials are of the same level of accuracy.

Shown in Fig. 2 are phonon dispersion curves under ambient pressure, and the high-symmetry points are defined in Table II. This figure shows clearly that there exists no imaginary frequency within the whole Brillouin zone, indicating that cg-N is metastable under ambient pressure. We also checked the result with a DFT molecular dynamics simulation, which confirms the metastability of cg-N under ambient pressure and up to a temperature of 500 K or even higher.

B. Surface decomposition paths and associated reaction barriers

When a three-dimensional infinite crystal meets a surface the periodicity of the crystal breaks at the surface. As a result the unsaturated surface atoms are more energetic and less stable than that of the bulk. Therefor we should take the surface stability into account when discussing the metastability of cg-N. Here we consider a series of surface decomposition processes occurring on the low-index (100), (110), and (111) surfaces. The processes are imaginary ones in which

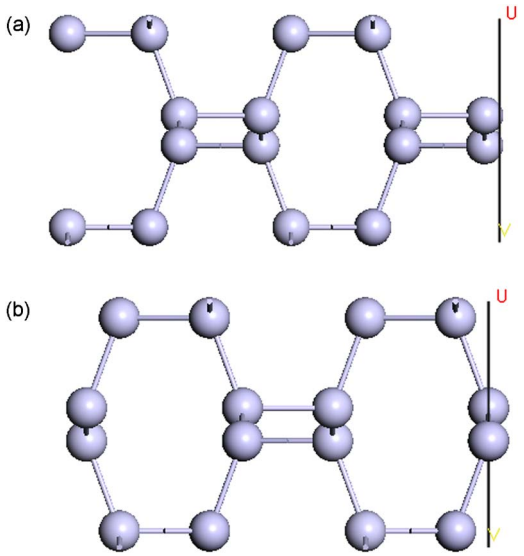

FIG. 4. (Color online) Two distinct subsurfaces associated with the (100) surface of cg-N. The two exposed surface atoms are respectively (a) 1 and 2 (subsurface I), and (b) 3 and 4 (subsurface II) as labeled in Fig. 3.

the energetic surface atoms break bonds that connect them to the bulk atoms, forming N_2 molecules and breaking away from the surface. Obviously the process is an energy favorable one, because of the large amount of energy released in the process in transforming from the single-bonded N atoms in cg-N to the triply bonded N_2 molecules. However, it should be pointed out that usually there exists an energy barrier associated with the process, this transition state or reaction barrier prevents the process from occurring, making the surface a metastable one.

For a particular (hkl) surface there exists possibly more than one subsurface as shown in Figs. 3–6 for the (100), (110), and (111) surfaces of cg-N. In Fig. 3 we see that subsurface I [Fig. 4(a)] may be obtained by cutting the lattice parallel to the (100) surface such that it exposes atoms 1 and

TABLE II. High-symmetry points in the Brillouin zone of cg-N. The wave vector **q** is given in terms of the lattice constant a and for a bcc lattice (Ref. 6).

Label	Wave Vector **q**
Γ	0
H	$\frac{2\pi}{a}(1,0,0)$
N	$\frac{\pi}{a}(1,1,0)$
P	$\frac{\pi}{a}(1,1,1)$

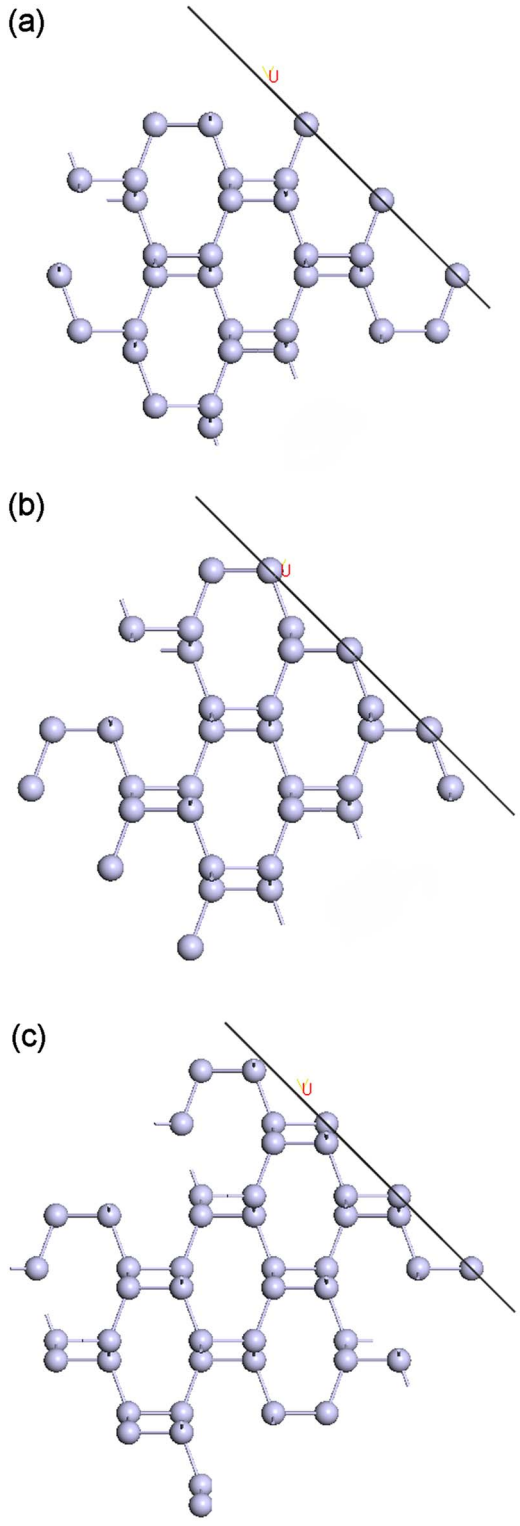

FIG. 5. (Color online) Three distinct subsurfaces associated with the (110) surface of cg-N. The two exposed surface atoms labeled in Fig. 3 are respectively (a) 2 and 6 for subsurface III, (b) 4 and 8 for subsurface IV, and (c) 1 and 5 for subsurface V.

2 on the surface. Subsurface II [Fig. 4(b)] is obtained by cutting through atoms 3 and 4. Subsurfaces associated with other surfaces may be obtained via the same way, and for the (110) surface there exist three nonequivalent subsurfaces

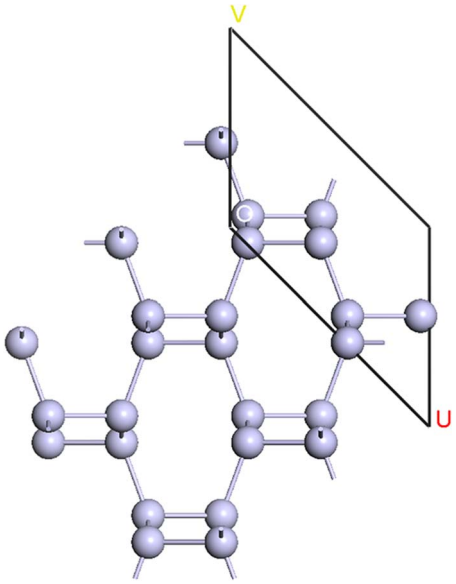

FIG. 6. (Color online) Subsurface VI associated with the (111) surface. The exposed three atoms are atoms 2,4,5 as labeled in Fig. 3, and atom 3 lies a little below the exposed surface atoms.

(Fig. 5) and for the (111) surface there exists only one such subsurface (Fig. 6).

When choosing the subsurfaces to investigate we follow the principle that surface decomposition processes would likely to occur on subsurfaces having the fewest number of bonds that would need to be broken to release nitrogen molecules from the surface. This is because the fewer the bonds to be broken, the lower the reaction barrier energy. For example in Fig. 3 atoms 3 and 4 are unlikely to break away directly from subsurface I to form a N_2 molecule. This is because there exist atoms 1 and 2 on top of them and the total number of bonds needing to be broken is four in order to release a N_2 molecule. This process is energetically unfavorable compared with the process in which atoms 1 and 2 break away from subsurface I to form a N_2 molecule, exposing the atoms 3 and 4 beneath (subsurface II). As the decomposition process continues, the whole subsurface I vaporizes to become nitrogen molecules converting subsurface I into subsurface II. The exposed atoms 3 and 4 on subsurface II then begin to break away from the exposed subsurface II, converting the surface back to subsurface I.

For transition state search calculations we employed a supercell method. The decomposition process can be simulated with one N_2 molecule releasing from the surface of a slab in one supercell. For the (100) and (110) surfaces, a 3×3 surface supercell is used for transition state search. For the (111) surface, a 2×2 surface supercell is used, because the (111) surface unit cell is larger than that of the (100) and (110) surfaces. With this standard supercell method, the distances between N_2 molecules released from different supercells are about 10 Å, and interaction between these N_2 molecules is negligible. For simulating vacuum, an empty space of 10 Å is inserted between the periodic cg-N slabs, and atoms at the bottom of the crystal slabs are fixed. It should be noted that the calculated results, such as the averaged total energy per N_2 molecule, depend on the the size of the supercell, and in

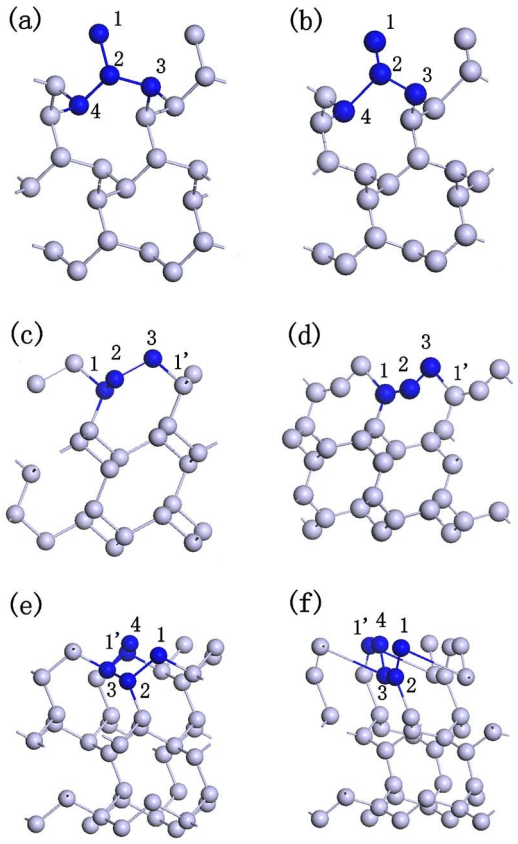

FIG. 7. (Color online) Atomic models of three as-cut and relaxed subsurfaces associated with the cg-N (110) surface. The (a) as-cut and (b) optimized subsurface III. The (c) as-cut and (d) optimized subsurface IV. The (e) as-cut and (f) optimized subsurface V.

particular depend on the thickness of the crystal slab. This effect may in principle be eliminated when an infinite crystal slab is used. However, in practical calculations we have to make a compromise between the limited computer resources and the computation accuracy. In this work we used a lower limit of 5 Å for the thickness of the cg-N slab in all our calculations, and found that this thickness gives a reasonably convergent result. Numerically we found that a thicker crystal slab normally results in a larger decomposition barrier; our following results on the transition state barrier provide therefore a underestimate of the true barrier, i.e., the surface is normally more stable than our calculated barrier for the crystal slab of finite thickness would suggest.

Explicitly we have used the following supercells in our calculations on possible decompositions occurring on the surfaces of cg-N. For the (100) surface the supercell is $11.44\times11.44\times15.04$ Å^3, with $\alpha=\beta=\gamma=90°$ (subsurface I, three layers) and $11.44\times11.44\times16.40$ Å^3, with $\alpha=\beta=\gamma=90°$ (subsurface II, four layers). For the (110) surface, the supercell is $9.91\times9.91\times17.61$ Å^3, with $\alpha=90°$, $\beta=90°$, $\gamma=70.52°$ (subsurfaces III and IV), $9.91\times9.91\times16.74$ Å^3, with $\alpha=90°$, $\beta=90°$, $\gamma=70.52°$ (subsurface V). For the (111) surface, the parameters for the 2×2 supercell are $10.77\times10.77\times15.81$ Å^3, with $\alpha=90°$, $\beta=90°$, $\gamma=120°$.

The transition state search is based on the process where two nearby N atoms on the top surface break away from the surface to form a N_2 molecule in vacuum. We carried out calculations as followed. First we optimized initial and final configurations of all decomposition paths to find energy minima, and then searched the potential hypersurface via reaction coordinates with a restricted conjugate gradient optimization method to find transition states and to confirm the reaction barriers. Our final results are summarized in Table III.

TABLE III. Decomposition paths and associated reaction barriers in eV per N_2 molecule released and the root mean square (rms) force of the transition state in eV/Å. The rms force of a real transition state should be zero, and here no rms force is greater than 0.16 eV/Å. The energy gain of all these decomposition pathways is about 2 eV per N_2 released.

Starting point	Surface	Barrier	rms force of TS
I	(1,0,0)	0.0742	0.0886
II	(1,0,0)	1.1500	0.0888
III	(1,1,0)	0.0827	0.0862
IV	(1,1,0)	0.1626	0.0958
V[a]	(1,1,0)	0.0755	
V relaxed[b]	(1,1,0)	0.0168	0.1577
VI	(1,1,1)	0.3822	0.0922
		0.1274[c]	

[a]There is a barrier in relaxing the as-cut surface to the chainlike configuration. The barrier results from the energy increase from the spin-polarized stable state to the spin-unpolarized excited state with the same atomic configuration. There is no reaction path involved in this step, so there is no rms force.
[b]After overcoming the spin barrier, the relaxation process to the N chain configuration is barrier-free. The second barrier is associated with the process in which the whole N chain breaks away.
[c]Barrier averaged by 3 N_2 molecules released in the process.

Shown in Fig. 4 are two subsurfaces associated with the (100) surface of cg-N. Subsurface I decomposes by releasing a N_2 molecule and exposing the subsurface II beneath. The decomposition barrier is 0.0742 eV/N_2. When the starting configuration is subsurface II, the barrier is 1.1500 eV/N_2. The two processes involve different barrier heights, and this difference results from the fact that the two subsurfaces involve different dangling bond configurations. It is clear that subsurface II is much more stable than subsurface I, and indeed it will be shown that subsurface II is the most stable surface among all the subsurfaces we examined.

In general after optimization the subsurfaces associated with the (110) surface of cg-N become very much distorted near the surface region (see Fig. 7). This fact indicates that these relaxed subsurfaces are highly strained and not very stable. For the three subsurfaces associated with the (110) surface, the decomposition processes are likely to occur as follows.

Subsurface III. The as-cut and fully relaxed surface structures are shown in Figs. 7(a) and 7(b), respectively. The two nitrogen atoms [atoms 1 and 2 in Figs. 7(a) and 7(b)] at the top of subsurface III overcome an energy barrier of 0.0827 eV/N_2 to form a N_2 molecule, and to expose the atoms on subsurface IV beneath. This energy barrier is quite

TABLE IV. Reaction barrier energy and the reaction energy for five subsurfaces with small decomposition barrier of about 0.1 eV/N_2. The subsurfaces are either bare or saturated by H atoms. Note that for different subsurfaces, the number of dangling bonds is not the same and the numbers of hydrogen atoms used to saturate the surfaces are different. The reaction barriers and reaction energies are given in eV per H_2 or N_2H_2 molecule formed in molecule-releasing cases, but eV per unit length for the N chain formed in subsurface V [see Fig. 7(f), with the unit length being the length of a N_2 dimer in the N chain].

Reactant	Product	Reaction barrier (eV)	Reaction energy (eV)
H-saturated I	H-saturated I minus 2N, 2H, and N_2H_2		0.802
H-saturated I	H-saturated I minus 2H and H_2		1.046
H-saturated III	H-saturated III minus 2N, 2H, and N_2H_2		2.402
H-saturated III	H-saturated III minus 2H and H_2		2.217
H-saturated IV	H-saturated intermediate of IV	0.187	−1.246[a]
H-saturated intermediate of IV	H-saturated intermediate of IV minus 2N, 2H, and N_2H_2		1.639[b]
H-saturated IV	H-saturated IV minus 2H and H_2		0.060[c]
H-saturated V	NH chain layer	0.529	−0.429
H-saturated V	H-saturated V minus 2H and H_2		3.243

[a]The decomposition pathway is similar to that of the the bare surface as described in the text. The first step is to break the longer bond, and this step is an exothermic one.

[b]The second step, which is to break the shorter bond, becomes an endothermic reaction due to the saturation effect of H atoms.

[c]The final configuration is also quite distorted so the reaction energy is quite low but still positive. Compared with the bare surface's energy gain (about 2 eV/N_2), the hydrogen-saturated surface is more stable.

low because in the relaxed subsurface III [Fig. 7(b)], the N_2 dimer formed by atoms 1 and 2 is weakly bonded to the bulk atoms 3 and 4, having bond lengths of 1.44 and 1.84 Å, respectively. These two bonds are much longer than that between the two atoms of the dimer, i.e., between atoms 1 and 2 (1.19 Å), indicating that the binding between this dimer and the surface is very weak. The dimer may easily break away from the surface to form an isolated N_2 molecule.

Subsurface IV. The as-cut and fully relaxed surface structures are shown in Figs. 7(c) and 7(d), respectively. The two top atoms (atoms 2 and 3) may break the two bonds connecting them to the bulk, i.e., the bonds between atoms 1 and 2, and 3 and 1′ (note that atom 1′ is equivalent to atom 1) and form a N_2 molecule. The two bonds (between atoms 1 and 2, and 3 and 1′) are stronger than that between the surface dimer and bulk atoms 3 and 4 on subsurface III [Figs. 7(a) and 7(b)], leading to a much higher reaction barrier for the direct decomposition. However, we found that the reaction may proceed via an alternative path with a much lower barrier. In this path the two bonds (i.e., between atoms 1 and 2, and 3 and 1′) break one after another, instead of breaking simultaneously. The longer bond between atoms 1′ and 3 [about 1.64 Å; see Fig. 7(d)] breaks first; the two atoms 3 and 2 form a N_2 dimer which then moves toward vacuum and turns a small angle around atom 1 to which the dimer is still bonded. The shorter bond (between atoms 1 and 2) then breaks, releasing a N_2 molecule. With this path, the reaction barrier is about 0.163 eV/N_2. This barrier is much lower than that associated with the direct flyaway path, but is still higher than that associated with subsurface III.

Subsurface V. The as-cut and fully relaxed surface structures are shown in Figs. 7(e) and 7(f), respectively. The decomposition path for this subsurface is complex. First the as-cut surface distorts to form a chainlike surface, which is shown in Fig. 7(f), and the top four atoms (1 to 4) become very weakly bonded to the bulk atoms beneath [Fig. 7(f)]. This chainlike structure has been predicted to be lower in energy than the cg-N structure under low pressure.[2] In this case, there exists a barrier associated with the excitation between different spin states of the atoms on subsurface V. When the atoms on the surface of Fig. 7(e) are excited from the spin-polarized stable state to a spin-unpolarized state with higher energy, there no longer exists any barrier for the surface to form a distorted chainlike structure as shown in Fig. 7(f). The spin barrier in the first step is about 0.076 eV/N_2. After overcoming the spin barrier, there exists only one bond connecting the four surface atoms in the N chain with bulk atoms beneath. The next step of the decomposition path is that the N-chain breaks away from the surface, and the barrier associated with this step is about 0.0168 eV/N_2. Note that the final breaking process is not associated with a single N_2 molecule but with the whole N chain. The numerical value of the barrier is therefore converted to eV per N_2 so that it can be compared with the barriers associated with other subsurfaces (see Table III).

Figure 6 shows subsurface VI associated with the (111) surface of cg-N. We considered two decomposition paths under ambient pressure. One is that the four near surface atoms 2,3,4,5 (as labeled in Fig. 3) all break away from subsurface VI. This process needs to break three bonds and form a phosphoruslike N_4 cluster. However, the energy of the N_4 cluster is quite high so that the reaction is an endothermic one. The energy needed to form a N_4 cluster is 1.781 eV, making the process a highly unlikely one. The other path is to release N_2 molecules directly from the surface. For example the reaction may be initiated by forming a N_2 molecule out of atoms 2 and 3 (as labeled in Fig. 3). The near-surface region is then left with four atoms which are all unstable. Two additional N_2 molecules may readily be formed and leave the surface without any barrier. The main reaction barrier is associated

with the first step and is 0.3822 eV, and the barrier averaged by three N_2 formed is 0.3822 eV/$(3\times N_2)$=0.1274 eV/N_2.

C. Surface stabilization by H atoms

Earlier calculations indicate that surfaces may play an important role in the stability of the cg-N crystal. Potential applications of this material may therefore be limited by the unstable character of its surfaces. One important question is therefore whether or not we can make the surface of cg-N more stable so that the material can be used under normal conditions. To answer this question we performed a comparative study on the bare and H-saturated subsurfaces. We focus our attention on the less stable subsurfaces whose decomposition barriers are about 0.1 eV/N_2 or less (i.e., subsurfaces I, III, IV, and V), and the results are listed in Table IV. A positive reaction energy implies that the reaction is an endothermic one. Since we are interested in the metastability of the surface, we did not consider the reaction barrier for endothermic reaction. When H atoms are present on the surface, these atoms may form bonds with dangling bonds on the surface and stable the surface. For subsurfaces I and III, adding hydrogen atoms will cause a direct stabilization of these surfaces. For subsurface IV, along the similar two-step decomposition pathway of the bare subsurface IV described earlier, adding hydrogen atoms will not increase the barrier of the first step, but will make the second step an endothermal one. Therefore, after overcoming a barrier of 0.187 eV/N_2H_2, the H-saturated subsurface IV will fall into a more stable intermediate configuration in which a single bond exists between a N_2H_2 cluster and the atoms beneath the surface. For the H-saturated subsurface V, the structure distortion occurring on the bare subsurface V as shown in Figs. 7(e) and 7(f) will be associated with a much higher barrier. The presence of H atoms on the surface helps the (100) and (110) surfaces to become a more stable one.

IV. CONCLUSIONS

We performed systemic *ab initio* calculations on the phonon dispersion curves of cg-N under ambient pressure and transition state barriers for surface decompositions on the (100), (110), and (111) surfaces of cg-N. Our results suggest that an infinite cg-N structure is mechanically metastable under ambient pressure and room temperature. Among the three low-index surfaces investigated we found that the (110) surface is the least stable, and the (100) surface (subsurface II) is the most stable. On the other hand, saturating the dangling bonds on the surface with H atoms can substantially stabilize the surface. These results point to the possible use of cg-N under ambient environment as, e.g., energy storage materials.

ACKNOWLEDGMENTS

This work was supported by the Ministry of Science and Technology (973 Grant No. 001CB610502, 863 Grant No. 2004AA302G11), National Science Foundation of China (Grant No. 10434010), the Chinese Ministry of Education (Grants No. 10401 and No. 2004036178), and the National Center for Nanoscience and Technology of China.

*Author to whom correspondence should be addressed. Email address: lmpeng@pku.edu.cn

[1] A. K. McMahan and R. LeSar, Phys. Rev. Lett. **54**, 1929 (1985).
[2] C. Mailhiot, L. H. Yang, and A. K. McMahan, Phys. Rev. B **46**, 14419 (1992).
[3] M. I. Eremets, A. G. Gavriliuk, I. A. Trojan, D. A. Dzivenko, and R. Boehler, Nat. Mater. **l3**, 558 (2004).
[4] M. I. Eremets *et al.*, J. Chem. Phys. **121**, 11296 (2004).
[5] M. Popov, Phys. Lett. A **334**, 317 (2005).
[6] T. W. Barbee III, Phys. Rev. B **48**, 9327 (1993).
[7] M. D. Segall *et al.*, J. Phys.: Condens. Matter **14**, 2717 (2002).
[8] J. P. Perdew, J. A. Chevary, S. H. Vosko, K. A. Jackson, M. R. Pederson, D. J. Singh, and C. Fiolhais, Phys. Rev. B **46**, 6671 (1992).
[9] D. R. Hamann, M. Schluter, and C. Chiang, Phys. Rev. Lett. **43**, 1494 (1979).
[10] D. Vanderbilt, Phys. Rev. B **41**, 7892 (1990).
[11] M. C. Payne, M. P. Teter, D. C. Allan, T. A. Arias, and J. D. Joannopoulos, Rev. Mod. Phys. **64**, 1045 (1992).
[12] S. Baroni, S. de Gironcoli, A. dal Corso, and P. Giannozzi, Rev. Mod. Phys. **73**, 515 (2001).
[13] T. A. Halgren and W. N. Lipscomb, Chem. Phys. Lett. **49**, 225 (1977).